Influence of Aquifer Heterogeneity on Cr(VI) Diffusion and Removal From Groundwater

Weidong Zhao
Hefei University of Technology School of Resources and Environmental Engineering
https://orcid.org/0000-0001-9008-2836

Xinxiang Huang
Hefei University of Technology School of Resources and Environmental Engineering

Jianshi Gong
China Geological Survey

Lei Ma (Lei8505@hfut.edu.cn)
Hefei University of Technology School of Resources and Environmental Engineering
https://orcid.org/0000-0003-3339-8740

Jiazhong Qian
Hefei University of Technology School of Resources and Environmental Engineering

Research Article

Keywords: Groundwater, Heterogeneity, Emulsified vegetable oil, Cr(VI) removal, Permeable reactive barrier, Biodegradation

Posted Date: April 23rd, 2021

DOI: https://doi.org/10.21203/rs.3.rs-373202/v1

Version of Record: A version of this preprint was published at Environmental Science and Pollution Research on August 16th, 2021. See the published version at https://doi.org/10.1007/s11356-021-15803-4.

Influence of aquifer heterogeneity on Cr(VI) diffusion and removal from groundwater

Weidong Zhao[a] , Xinxiang Huang[a], Jianshi Gong[b], Lei Ma[a,*], Jiazhong Qian[a]

[a,*] School of Resources and Environmental Engineering, Hefei University of Technology, Hefei, 230009, China

[b] Nanjing Geological Survey Center, China Geological Survey, Nanjing, 210016, China

Corresponding authors:

Lei Ma

School of Resources and Environmental Engineering, Hefei University of Technology, Hefei City, 230009, China

Tel: +86 136 3706 7509; Fax: +8655162901523;

E-mail addresses: Lei8505@163.com; Lei8505@hfut.edu.cn

Abstract

Previous studies show aquifer heterogeneity has an important influence on removal of Cr(VI) in groundwater, but little research has revealed the role of aquifer heterogeneity in Cr(VI) migration and how effective using emulsified vegetable oil is for Cr(VI) removal in groundwater. We simulated a laboratory sand-packed box over a 50-day period to research the effects of aquifer heterogeneity on Cr(VI) diffusion and also injected emulsified vegetable oil (EVO) into the permeable reactive barrier (PRB) filled with compost to investigate the influences of aquifer heterogeneity on Cr(VI) removal from groundwater, with fixed conditions of simulated true water temperature of shallow groundwater (19±0.5 ℃), hydraulic gradient (3‰), the Suzhou coal mining area (Anhui, China). The results show that aquifer heterogeneity had the significant impact on Cr(VI) diffusion with an overall diffusion direction of Cr(VI) that was from the upper left corner to the lower right corner along the direction of the groundwater; permeable reactive barrier would effectively remove Cr(VI) from groundwater in heterogeneous aquifer due to the vertical movement of microorganisms between different aqueous media; coarse sand and medium sand showed high performance in Cr(VI) diffusion, with a slight superiority to fine sand; following a one-time EVO injection, a considerably stable and uniform effective remove zone similar to the shape of ∑ was formed in the heterogeneous aquifer, and its Cr(VI) removal efficiency was over 95%.

Keywords:

Groundwater; Heterogeneity; Emulsified vegetable oil; Cr(VI) removal; Permeable reactive barrier; Biodegradation

1. Introduction

Chromium is one of the most frequently detected heavy metals in groundwater, surface waters and industrial sites, which has been considered as one of the top 20 contaminants on the superfund priority list of hazardous substances for the past 15 years (Grabarczyk et al. 2006). Numerous industrial applications, such as production of alloys and mainly steel production, metal finishing, electroplating, leather tanning, textile synthesis, wood treatments and coal mining, usually cause chromium contaminated groundwater (Guo et al. 2011, Sahinkaya &Kilic 2014, Yoon et al. 2011). The ground within the Suzhou coal mine area (Huaibei coal mine area, northern Anhui Province, China) has subsided to varying degrees due to long-term and large-scale coal mining, and shallow pipeline has formed a relatively uniform drop funnel, which means coal mining has severely changed the flow field of the shallow pipeline. Besides, existing studies have shown that mine drainage, gangue piles and collapse ponds formed by long-term coal mining poses a serious threat to surface water, groundwater and soil. In particular, the shallow groundwater has been polluted by conventional components such as ammonia nitrogen and heavy metals such as Cr(VI) (Peng &Sun 2014). Cr(VI) is highly toxic to humans, animals, plants and microorganisms and is associated with the development of various chronic health disorders including organ damage, dermatitis and respiratory impairment (Xu et al. 2004), which has been classified as a Group A human carcinogen by the U.S. Environmental Protection Agency (EPA) (Dhal et al. 2013). Therefore, Cr(VI)

contaminated treatment has attracted more and more attention. Recently the permeable reactive barrier (PRB), with a low cost and an effective treatment in contaminated groundwater remediation, has been widely studied and applied (Thiruvenkatachari et al. 2008).

The PRB is an effective technology for in situ remediation of Cr(VI) contaminated groundwater in the field (Blowes et al. 1997), the key part of which is the reactive media filled in PRB and the reaction zone formed. The most applied reactive media in PRB are zero-valent iron (ZVI) (Cang et al. 2009, Fu et al. 2014, Qiu et al. 2020, Wei et al. 2016, Weng et al. 2007), activated carbons (Huang et al. 2015, Song et al. 2019, Su et al. 2019), zeolites (Buenano et al. 2017, Kesraoui-Ouki et al. 1993, Li et al. 2014, Peric et al. 2004), bentonite (Wang et al. 2020, Zhang et al. 2012) and emulsified vegetable oil (EVO) (Harkness &Fisher 2013, Watson et al. 2013, Wen et al. 2017). EVO is an important biodegradable reactive media filled in PRB technology for Cr(VI) reduction. It could stably form a large-scale microbial reaction zone for a long period. Several scholars found that the effective migration distance of emulsified oil in the aquifer could reach 8 m, which could create an effective reaction zone within a certain range (Borden 2007, Boris et al. 2008, Clayton &Borden 2009). Emulsified oil particles adsorbed on the surface of reactive media could function stably in 3-5 years (Hughes 2007).

Previous studies have shown that emulsified vegetable oil (EVO) (Hiortdahl &Borden 2014) and aquifer heterogeneity have a significant effect on removing Cr(VI) from groundwater. EVO, replacing organic matter (volatile solids, VS), is well distributed in the sandbox after was injected into a corner of a sandbox that had heterogeneous layered layers of fine-medium-coarse sand (from top to bottom) (Jung et al. 2006). A one-time injection of EVO or amended EVO could effectively induce the occurrence of dissimilatory iron reduction, and microbial activity is responsible for the process, showing feasibility to remove Cr(VI) from groundwater (Wen et al. 2017). EVO has proven efficient for anaerobic bioremediation of acid mine drainage for 300 days in column tests (Lindow &Borden 2005). Effluent concentrations from PRBs in heterogeneous aquifers tend to be greater than effluent concentrations predicted using the conventional one-dimensional deterministic plug flow model typically used for design (Elder et al. 2002). The effects of geologic heterogeneities in an aquifer containing an embedded clay lens and those of stratified aquifer that comprises two geologic formations, on the remediation of an organic contaminated aquifer through stochastic analysis (Lee et al. 2000).

Researchers used plexiglass sand columns or three-dimensional sandboxes to carry out indoor experiments on the simulated restoration of Cr(VI) pollution in groundwater and obtained a series of research results. To assess a reactive zone with emulsified vegetable oil for the long-term remediation of Cr(VI)-contaminated aquifer, experiments were carried out in a three-dimensional plexiglass sandbox with

86 fixed conditions of constant temperature (15.5 °C), hydraulic gradient (4‰), and
87 simulated groundwater flow rate (10 cm/d) (Dong et al. 2018). In order to investigate
88 the possibility of using the four considered materials (Fe^0, Fe^0/Cu, AC and S/Z) inside
89 PRB for Cr(VI) from groundwater, four packed-column experiments were conducted.
90 A plexiglass column, with dimensions of 20 cm length and 2.5 cm inner diameter, was
91 used for packing the materials (Maamoun et al. 2020). The transport of Cr(VI) in the
92 presence of bentonite colloidal particles was studied in an experimental column filled
93 with sand, of which plexiglass column with a length of 50 cm, an inner diameter of 4.8
94 cm, and the outer diameter of 5 cm (Ghiasi et al. 2020).

95 In summary, previous studies have mostly focused on the effective diffusion
96 distance of emulsified vegetable oil, reactive media in PRB, service life and
97 removal effect, etc, but there have been no detailed reports about the influence
98 of heterogeneous aquifers of groundwater on Cr(VI) migration and Cr(VI)
99 removal from groundwater by emulsified vegetable oil. Also, previous
100 laboratory experiments were generally carried out at room temperature and
101 experimental conditions such as the actual water temperature and hydraulic
102 gradient of the groundwater in the field were not fully considered, which made
103 it difficult to apply the results of indoor experiments in situ remediations of
104 Cr(VI) contaminated groundwater in the field. In this study, we simulated a
105 laboratory-scale sandbox to examine the influence of aquifer heterogeneity on Cr(VI)
106 diffusion and also simulated PRB filled with compost and one-time EVO injection to

investigate the effectiveness of Cr(VI) removal, with fixed conditions of simulated true water temperature of shallow groundwater (19±0.5 ℃), hydraulic gradient (3‰), the Suzhou coal mining area (Anhui, China).

2. Materials and methods

2.1. Materials

EVO was prepared by blending 60% vegetable oil, 13% surfactant, and 27% water with a booster mixer at 3000 rpm constant stirring for 10 minutes, put in a 55 °C water bath for 10 minutes, taken out, cooled naturally to room temperature, and stored in a cool place after sealing. The compost (purchased in a flower market) was stored in a cool, ventilated and dry place. The sand was purchased from a building materials market, dried after carefully sieved in a standard wire sieve and made into coarse, medium, and fine sand according to the ratio shown in Table 1, respectively. Table 1 describes the characteristics of packed sand in the diffusion and removal study. The simulated Cr(VI) contaminated groundwater sample with a 20 mg/L concentration (Li et al. 2019, Lv et al. 2019), which was prepared with potassium dichromate (excellent grade pure) and deionized water.

2.2. Experiment equipment

A three-dimensional sandbox composed of plexiglass was used in this study. The plexiglass sandbox (90 cm in length, 25 cm in width, and 48 cm in height) was composed of an inlet tank, stratified aquifers (coarse, medium and fine sand), PRB, injection well (a plexiglass column), outlet tank and other auxiliary equipment in order from left to right as shown in Fig. 1. Fig. 1 shows the detailed experimental design. There were 18 sampling ports from the front glass of the box, one water inlet and one water outlet from each side of the box. The sampling ports were both laid every 10 cm horizontally from left to right (6 columns), and every 10 cm vertically from bottom to top (3 rows). Each sampling port was a plexiglass column (5 mm in inner diameter) inserted into the sandbox 12 cm. One port of plexiglass columns was wrapped with gauze inside the sandbox and the other port was connected with a rubber tube, of which clamps stopped the rubber tube from water. There was 15 cm of fine sand, 15 cm of medium sand and 13 cm of coarse sand were packed sequentially from bottom to top. The sand finally reached a level of 43 cm and 2 cm of wet clay was used to cover its surface tightly for reducing water evaporation. PRB (25 cm in length, 20 cm in width, 43 cm in height) was laid 15.5 cm away from the right side of the water inlet, and the filled reactive media was a mixture of quartz sand and compost (4 g). After each 5-cm lift, filled reactive media was repeatedly compacted using a wooden stick to ensure the homogeneity of each filling. In this way, both sides of the

PRB in the sandbox were packed with sand as the heterogeneous aquifer media. A glass tube with holes all around was buried in the center of the PRB to simulate an injection well in the field.

After the filling was completed, tap water was injected into the sandbox through a peristaltic pump, and the aquifer was saturated with water by standing for two days. Then, the rate of the peristaltic pump and outlet height were set to maintain the inlet water level at 40 cm under the condition that the starting point of the water level was the bottom surface of the water body at the inlet end, the pore water flow rate was 10 cm/d, and the hydraulic gradient was 3‰.

2.3. Experimental method

Contaminated groundwater containing 20 mg/L of Cr(VI) replaced tap water as a continuous water inflow after the water level of the sandbox stabilized. Meanwhile, a glass rod was used to immediately and rapidly agitate the water body in the inlet tank so that Cr(VI) contaminated groundwater uniformly filled throughout the whole inlet tank, making it a typical source of lateral runoff pollution. It was the first day that the experiment officially began.

The experiment lasted for 25 days from November 22 to December 18, 2019 (stage 1) with conditions of hydraulic gradient constant (3‰) and groundwater temperature (19±0.5 °C). During stage 1, water samples were collected from

sampling ports at 9 am every day. When the concentration of Cr(VI) of all water samples reached a maximum value and remained stable for five days, we believed there formed a stable Cr(VI) contaminated groundwater chemical field in the sandbox aquifer. After that, a one-time injection of 8 L of emulsified vegetable oil (5 g/L) was into the aquifer at a rate of 1500 mL/h by a peristaltic pump through the injection well. With the other experimental conditions unchanged, the experiment continued for 23 days from December 19, 2019 to January 10, 2020 (stage 2). During stage 2, water samples were collected at 7 o'clock every evening, and its Cr(VI) concentration was determined by the 1,5 diphenylcarbohydrazide spectrophotometric method. When Cr(VI) concentration of all water samples was 0 mg/L or reached a minimum value and remained unchanged for 5 days, the experiment completed.

3. Results and discussion

3.1. Effect of aquifer heterogeneity on Cr(VI) diffusion in groundwater

A hill-shading profile of Cr(VI) concentration distribution in each water sample of the heterogeneous aquifer corresponding to the I-I' section (stage 1) was generated using the Kriging interpolation function in ArcGIS 10.1 software, showing diffusion characteristics of Cr(VI) in heterogeneous aquifers on different days during stage 1 (Fig. 2). In this figure, the aquifers are coarse, medium and fine sand from top to bottom, respectively, the direction of water flow is from left to right, the PRB is X-axis coordinate range from 7.5 cm to 27.5 cm, and different gradient colors from off-white to red indicate the concentration of Cr(VI) from the low to the high.

Cr(VI) contaminants continuously diffused after entering heterogeneous aquifers (Fig. 2), and the rate of horizontal diffusion was significantly faster than vertical diffusion. Specifically, we studied the diffusion characteristics of Cr(VI) contaminants in heterogeneous stratified aquifers by taking the orange zone (OZ) (Fig. 2) as an example, where Cr(VI) concentration was equal to or over 16 mg/L and less than 18 mg/L. Generally, the OZ mainly spread rapidly to the right in the horizontal direction, but slowly downward in the vertical direction. The results indicate the OZ usually diffused from the upper left corner to the lower right corner along the direction of the groundwater flow. Also, Fig.

194 2 depicts that the diffusion characteristics of the OZ changed gradually over
195 time in a single homogeneous aqueous media. On day 1 to 2, the OZ migrated
196 in the direction of groundwater flow, entering the PRB of coarse sand and
197 medium sand. Owing to the uneven concentration of Cr(VI) contaminated
198 groundwater in the inlet tank, Cr(VI) diffused horizontally in the coarse sand
199 slightly slower than in the upper part of the medium sand, but its horizontal
200 diffusion rate in coarse sand and medium sand was still much faster than in fine
201 sand. Simultaneously, diffusion rates of Cr(VI) changed with the time the OZ
202 migrated to the water outlet (Fig. 2). The OZ reached the top border of coarse
203 sand, medium sand and fine sand for the first time in 3, 5 and 14 days,
204 respectively, and migrated to the bottom of each homogeneous aqueous media
205 for the first time in 5, 14 and 17 days, respectively. The results show that Cr(VI)
206 diffusion rates in aqueous media with different permeability were distinct, of
207 which the fastest was in coarse sand, the second was in medium sand, and the
208 slowest was in fine sand. The horizontal diffusion rates of Cr(VI) in coarse sand,
209 medium sand and fine sand were calculated to be 0.054 m/d, 0.036 m/d and 0.018 m/d,
210 respectively, and Cr(VI) concentration of the entire heterogeneous aquifer almost
211 reached 20 mg/L at the end of stage 1.

3.2. Effect of aquifer heterogeneity on Cr(VI) removal effect

The distribution of Cr(VI) removal efficiency in the sandbox on different days was produced by the Kriging interpolation method during stage 2 shown in Fig. 3, which can show the distribution of Cr(VI) removal efficiency in the heterogeneous aquifer after EVO injection. The different gradient colors from dark blue to red indicate Cr(VI) removal efficiency from high to low in the figure.

Before injecting EVO (after stage 1 and before stage 2), Cr(VI) removal efficiency of the entire heterogeneous aquifer was basically zero (Fig. 3). At 7 pm on day 27, a one-time injection of 8 L of EVO (5 g/L) accompanied with carbon source facilitated microorganisms performance in the PRB on Cr(VI) removal. In order to describe Cr(VI) removal effect of the entire heterogeneous aquifer more conveniently, the zone of Cr(VI) removal efficiency above 95% was defined as the ERZ (effective removal zone) in this paper. The ERZ is the light blue and dark blue zones in Fig. 3. On day 28 to 45, whether it is seen from the entire heterogeneous aquifer or the inside of a single sand layer, similar to Cr(VI) diffusion in aquifers, diffusion of the ERZ was basically consistent with the overall flow direction of groundwater. On day 46 to 50, there formed a spatially stable ERZ. The results show that the groundwater flow field has an important effect on the spatial distribution of the ERZ, and a stable ERZ could

232 be finally established in the entire heterogeneous aquifer downstream of the
233 injection well 18 days following EVO injection under the experimental
234 conditions. The stable ERZ was approximately 38 cm in length, 40 cm in height,
235 covered 1520 cm^2, its removal efficiency remained 97% approximately, and its
236 stable time was not less than five days.

237 The spatial distribution and diffusion characteristics of the ERZ were quite
238 different within the heterogeneous aquifer composed of coarse sand, medium
239 sand and fine sand. The longest and shortest distances between the ERZ and the
240 injection well in three sand layers are shown in Fig. 4. And Fig. 5 depicts the
241 area changes of the ERZ in sand layers.

242 As shown in Fig. 3, on day 28 to 29 (stage 2), the left border (that is, the shortest
243 distance in coarse sand in Fig. 4) of the ERZ reached the right border of the
244 injection well (about 20 cm from the right side of the water inlet), the right
245 border (the longest distance in coarse sand) of the ERZ reached the right edge
246 of the coarse sand (60 cm from the right side of the water inlet), and the ERZ
247 diffused throughout the entire coarse sand except for a small area in the lower
248 right corner of coarse sand; The left edge (the shortest distance in medium sand)
249 of the ERZ reached the right border of the injection well, the right boundary
250 (the longest distance in medium sand) of the ERZ only reached the middle of
251 the medium sand (about 42 cm from the right side of the water inlet) and spread

252 vertically as far as the bottom of the medium sand (about 18 cm from the bottom
253 of the sandbox), whereas, the ERZ did not diffuse into the fine sand. The results
254 indicate that the microorganisms in the compost filled in the PRB could
255 effectively remove Cr(VI) in a certain range downstream of the injection well
256 after obtaining the carbon source of EVO.

257 The ERZ generally diffused upward and to the upper right in coarse sand and
258 medium sand, but the top right corner of the ERZ in coarse sand tended to
259 spread to the upper left. This tendency was most obvious on day 30 when the
260 ERZ first diffused into the left side of the PRB upstream of the injection well
261 (about 10 cm from the right side of the water inlet) and almost filled the entire
262 coarse sand in the PRB. Besides, a small portion of the ERZ also appeared in
263 medium sand. The ERZ in the coarse sand had shrunk downstream of the injection
264 well on day 31 and diffused upstream of the injection well at the end of stage 2.
265 Whereas, the ERZ in the fine sand did not spread to the upstream of the injection well
266 during stage 2. On day 30, the ERZ in fine sand first appeared in the middle of
267 the PRB and spread around, and it finally merged with the ERZ in coarse sand and
268 medium sand on day 32, forming a unified ERZ in the heterogeneous aquifer (the ERZ
269 below, unless otherwise specified to the unified ERZ). Its shape resembled a pistol
270 with the muzzle pointing to the right.

271 On day 33 to 34, the morphology of the ERZ did not change much, but its area
272 changed slightly. The ERZ covered a local maximum area of 901.97 cm^2 on
273 day 34 (Fig. 5). Furthermore, the left and right boundaries of the ERZ generally
274 extended from the upper left corner to the lower right corner along the direction
275 of water flow on day 35. The area of the ERZ in the whole heterogeneous
276 aquifer decreased drastically due to the significant decrease of which in the
277 coarse sand and reached a minimum local area (559.87 cm^2) on day 38. The left
278 edge of the EZR expand upstream and towards the PRB, while the right edge
279 of which kept spreading to the left bottom, and the area of the EZR started to
280 oscillate and increase gradually on day 39, reached a maximum area of 1357.87
281 cm^2 on day 47, and remained unchanged until the end of stage 2. Finally, the
282 ERZ was approximately in the shape of Σ, the left border of which was located
283 on the left side of the right border of the PRB. The ERZ filled the whole region
284 except for a small part in the fine sand at the lower left where was the entire
285 heterogeneous aquifer downstream of the right border of the PRB. The results
286 show that the EZR in the coarse sand rapidly covered the largest area 7 days
287 after EVO injection early in the experiment, but its area was rapidly reduced to
288 the smallest one in the following 2 days, and then it gradually increased due to
289 the interaction of microorganisms in medium sand and fine sand. Although the
290 area of the ERZ in medium sand and fine sand also fluctuated, the area of that
291 in the entire heterogeneous aquifer increased gradually and reached the

maximum value simultaneously with coarse sand at the end of stage 2 (Fig. 5). This indicates that microorganisms in coarse sand, medium sand and fine sand could have mutual flow vertically and form a stable and unified ERZ at the end of the experiment. Meanwhile, aquifer heterogeneity had the least impact on the ERZ.

Fig. 6, Fig. 7 and Fig. 8 show the variation of Cr(VI) removal efficiency over time in the sampling ports of coarse sand, medium sand and fine sand, respectively. Cr(VI) removal efficiency was calculated for the four materials using Eq. (1)(Maamoun et al. 2020)

$$Removal\ efficiency = \frac{C_0 - C_d}{C_0} \times 100\ (\%)$$

where, C_0 and C_d are initial concentration and concentration at time d of Cr(VI), respectively. The removal efficiency of Cr(VI) from the left to right 6 sampling ports in the coarse sand were represented as C1-C6, and the representatives of other sampling ports could be deduced by analogy.

On day 34, the removal efficiencies of Cr(VI) of coarse sand were basically stable at 90% after EVO injection except sampling port C1 (Fig. 6). Sampling port C1 was located at the center of the PRB and was close to the pollution source, which would result in a low Cr(VI) removal efficiency. Due to the faster water flow rate in the coarse sand and the more significant loss of

311 microorganisms and EVO, Cr(VI) removal efficiency of each sampling port
312 showed a decline tend downgradient on day 35, especially that of sampling port
313 C2 dropped to 40%, a considerable reduction in Cr(VI) biotransformation
314 efficiency. However, in the next 6 days, Cr(VI) removal efficiency of each
315 sampling port continuously increased, especially that of sampling port C2 rose
316 to 90% on day 41. Cr(VI) removal efficiency of the whole coarse sand
317 eventually reached equilibrium with around 90%, except that of sampling port
318 C1 was stable at 13% at end of stage 2.

319 As presented in Fig. 7, on day 32, the Cr(VI) removal efficiencies of sampling
320 ports M2 to M5 of medium sand exceeded 90%. Two sampling ports with
321 removal efficiency approaching 25% to 30% appeared. One of these was
322 sampling ports M6 mainly for a long distance from the PRB, fewer
323 microorganisms and nutrients, and the other was sampling ports M1 due to its
324 location in the upstream direction of the injection well. The Cr(VI) removal
325 efficiency of sampling ports M6 increased to 90% but that of sampling ports
326 M2 decreased from 90% to 20% on day 35 and kept fluctuating until it reached
327 equilibrium with 90% approximately on day 45. The variation of Cr(VI)
328 removal efficiency in the sampling ports of medium sand was similar to that of
329 coarse sand, except that the time of its overall Cr(VI) removal efficiency
330 recovered to 90% was 4 days later compared with coarse sand. The Cr(VI)

331 removal efficiencies of sampling port M2 to M6 were finally over 90% steadily,
332 only that of sampling port M1 was 12% steadily at the end of stage 2.

333 On day 35, the Cr(VI) removal efficiencies of sampling port F1, F5 and F6 were
334 below 20% while that of sampling port F3 and F4 of fine sand stabilized at 90%.
335 The Cr(VI) removal efficiencies of sampling port F5 and F6 slowly increased
336 and finally stabilized at 90% on day 45. The removal efficiency of sampling
337 port F2 rose slowly from 50% on day 29, and it fluctuated at 37% to 90% on
338 day 33 to 45 and recovered to 90% on day 47. The variation of Cr(VI) removal
339 efficiency in the sampling ports of fine sand was similar to that of medium sand,
340 except that the time of its overall Cr(VI) removal efficiency recovered to 90%
341 was 2 days later compared with medium sand. Finally, the removal efficiency
342 of Cr(VI) of sampling port F1 was stable at 13%, and that of other sampling
343 ports were stabilized at more than 90%, as illustrated in Fig. 8.

344 The above results indicate that under the experimental conditions, aquifer
345 heterogeneity significantly induced a change of removal efficiency of Cr(VI) in
346 each sand layer. The removal efficiencies of Cr(VI) of sampling port C2, M2
347 and F2 all decreased to varying degrees on day 35 and recovered to about 90%
348 on day 41, 45, and 47, respectively. This could be due to the vertical migration
349 of Cr(VI) contaminants in the three aqueous media with different permeability.
350 Following this, Cr(VI) removal efficiencies of the three aqueous media

351 decreased at different levels owing to microbial degradation and diffusion of
352 Cr(VI) contaminants. When Cr(VI) removal efficiency of fine sand was
353 exceedingly higher than that of medium sand and coarse sand, the migration of
354 Cr(VI) contaminants from fine sand to medium sand and coarse sand would be
355 aggravated. After that, on day 47, Cr(VI) removal efficiencies of the entire
356 heterogeneous aquifers were almost equal and stable at 90% ± 5% (except that
357 of sampling port C1, M1 and F1), indicating that aquifer heterogeneity at this
358 time had a minimal impact on the removal of Cr(VI).

359 ## 4. Conclusion

360 In this study, we investigated a simulated ERZ (effective reactive zone) for the in situ
361 bioremediation of Cr(VI) contaminated groundwater under simulated conditions of
362 hydraulic gradient (3‰), shallow groundwater temperature (19±0.5 °C), Suzhou coal
363 mining area (Anhui, China). Results revealed that coarse sand and medium sand
364 showed high performance in Cr(VI) diffusion, with a slight superiority to fine
365 sand, with final horizontal diffusion rates values of 0.054 m/d, 0.036 m/d and
366 0.018 m/d, respectively. Meanwhile, Cr(VI) horizontal diffusion was faster than
367 vertical diffusion in the entire heterogeneous aquifer or the single relatively
368 homogeneous aqueous media. The diffusion of Cr(VI) in the vertical direction
369 could make the entire heterogeneous aquifer polluted. Furthermore, Cr(VI)

overall diffusion direction was from the upper left corner to the lower right corner along the direction of groundwater flow.

Following EVO injection, a stable and uniform effective reactive zone(ERZ) similar to the shape of ∑ was formed in the heterogeneous aquifer downstream of the injection well. The ERZ almost filled the entire heterogeneous aquifer at the right boundary of the PRB, and its maximum area of section I-I' reached 1357.87 cm^2. The results showed that aquifer heterogeneity had the apparently significant influence on Cr(VI) removal efficiency of coarse sand, medium sand and fine sand, especially the removal efficiency in the horizontal direction. Due to the vertical diffusion between coarse sand, medium sand and fine sand, the microorganisms in different sand layers could flow to each other, resulting in an effective Cr(VI) removal in the entire heterogeneous aquifer.

Acknowledgments

This research was supported by the Program for the Geological Survey of China (No. DD20190354), the National Natural Science Foundation of China (No. 42072276), the National Key Natural Science Foundation of China (No. 41831289).

References

Blowes DW, Ptacek CJ, Jambor JL (1997): In-Situ Remediation of Cr(VI)-Contaminated Groundwater Using Permeable Reactive Walls: Laboratory Studies. Environ Sci Technol 31

Borden RC (2007): Effective distribution of emulsified edible oil for enhanced anaerobic bioremediation. J Contam Hydrol 94, 1-12

Boris F et al. (2008): In situ long-term reductive bioimmobilization of Cr(VI) in groundwater using hydrogen release compound. Environ Sci Technol 42, 8478-85

Buenano X, Canoira L, Martin Sanchez D, Costafreda J (2017): Zeolitic tuffs for acid mine drainage (AMD) treatment in Ecuador: breakthrough curves for Mn(2+), Cd(2+), Cr(3+), Zn(2+), and Al(3+). Environ Sci Pollut Res Int 24, 6794-6806

Cang L, Zhou D-M, Wu D-Y, Alshawabkeh AN (2009): Coupling Electrokinetics with Permeable Reactive Barriers of Zero-Valent Iron for Treating a Chromium Contaminated Soil. Separation Science and Technology 44, 2188-2202

Clayton MH, Borden RC (2009): Numerical modeling of emulsified oil distribution in heterogeneous aquifers. Ground Water 47, 246-58

Dhal B, Thatoi HN, Das NN, Pandey BD (2013): Chemical and microbial remediation of hexavalent chromium from contaminated soil and mining/metallurgical solid waste: a review. J Hazard Mater 250-251, 272-91

Dong J, Jinqiu Y, Qiburi B (2018): Simulated reactive zone with emulsified vegetable oil for the long-term remediation of Cr(VI)-contaminated aquifer: dynamic evolution of geological parameters and groundwater microbial community. Environ Sci Pollut Res Int 25, 34392-34402

Elder CR, Benson CH, Eykholt GR (2002): Effects of heterogeneity on influent and effluent concentrations from horizontal permeable reactive barriers. Water Resources Research 38, 27-1-27-19

Fu F, Dionysiou DD, Liu H (2014): The use of zero-valent iron for groundwater remediation and wastewater treatment: a review. J Hazard Mater 267, 194-205

Ghiasi B, Niksokhan MH, Mahdavi Mazdeh A (2020): Co-transport of chromium(VI) and bentonite colloidal particles in water-saturated porous media: Effect of colloid concentration, sand gradation, and flow velocity. J Contam Hydrol 234, 103682

Grabarczyk M, Korolczuk M, Tyszczuk K (2006): Extraction and determination of hexavalent chromium in soil samples. Anal Bioanal Chem 386, 357-62

Guo X, Fei GT, Su H, De Zhang L (2011): High-Performance and Reproducible Polyaniline Nanowire/Tubes for Removal of Cr(VI) in Aqueous Solution. The Journal of Physical Chemistry C 115, 1608-1613

Harkness M, Fisher A (2013): Use of emulsified vegetable oil to support bioremediation of TCE DNAPL in soil columns. J Contam Hydrol 151, 16-33

Hiortdahl KM, Borden RC (2014): Enhanced reductive dechlorination of tetrachloroethene dense nonaqueous phase liquid with EVO and Mg(OH)2. Environ Sci Technol 48, 624-31

Huang T, Li D, Kexiang L, Zhang Y (2015): Heavy metal removal from MSWI fly ash by electrokinetic remediation coupled with a permeable activated charcoal reactive barrier. Sci Rep 5, 15412

Hughes CM (2007): Effective Distribution of Injected Emulsified Oil for InSitu Bioremediation of Heterogeneous Aquifers. Norwegian Journal of Geology 92, 175-186

Jung Y, Coulibaly KM, Borden RC (2006): Transport of Edible Oil Emulsions in Clayey Sands: 3D Sandbox Results and Model Validation. Journal of Hydrologic Engineering 11, 238-244

Kesraoui-Ouki S, Cheeseman C, Perry R (1993): Effects of conditioning and treatment of chabazite and clinoptilolite prior to lead and cadmium removal. Environ Sci Technol 27, 1108-1116

Lee MK, Saunders JA, Wolf LW (2000): Effects of Geologic Heterogeneities on Pump-and-Treat and In Situ Bioremediation: A Stochastic Analysis. J Environmental Engineering Science 17, 183-189

Li S, Huang G, Kong X, Yang Y, Liu F, Hou G, Chen H (2014): Ammonium removal from groundwater using a zeolite permeable reactive barrier: a pilot-scale demonstration. Water Sci Technol 70, 1540-7

Li Z, Xu S, Xiao G, Qian L, Song Y (2019): Removal of hexavalent chromium from groundwater using sodium alginate dispersed nano zero-valent iron. J Environ Manage 244, 33-39

Lindow NL, Borden RC (2005): Anaerobic Bioremediation of Acid Mine Drainage using Emulsified Soybean Oil. Mine Water & the Environment 24, 199-208

Lv D, Zhou J, Cao Z, Xu J, Liu Y, Li Y, Yang K, Lou Z, Lou L, Xu X (2019): Mechanism and influence factors of chromium(VI) removal by sulfide-modified nanoscale zerovalent iron. Chemosphere 224, 306-315

Maamoun I, Eljamal O, Falyouna O, Eljamal R, Sugihara Y (2020): Multi-objective optimization of permeable reactive barrier design for Cr(VI) removal from groundwater. Ecotoxicol Environ Saf 200, 110773

Peng W, Sun L (2014): Heavy metals in shallow groundwater of the urban area in Suzhou, northern Anhui Province, China. Water Practice and Technology 9, 197-205

Peric J, Trgo M, Vukojevic Medvidovic N (2004): Removal of zinc, copper and lead by natural zeolite-a comparison of adsorption isotherms. Water Res 38, 1893-9

Qiu Y, Zhang Q, Gao B, Li M, Fan Z, Sang W, Hao H, Wei X (2020): Removal mechanisms of Cr(VI) and Cr(III) by biochar supported nanosized zero-valent iron: Synergy of adsorption, reduction and transformation. Environ Pollut 265, 115018

Sahinkaya E, Kilic A (2014): Heterotrophic and elemental-sulfur-based autotrophic denitrification processes for simultaneous nitrate and Cr(VI) reduction. Water Res 50, 278-86

Song Y, Wang L, Lv B, Chang G, Jiao W, Liu Y (2019): Removal of trace Cr(VI) from aqueous solution by porous activated carbon balls supported by nanoscale zero-valent iron composites. Environ Sci Pollut Res Int 27, 7015-7024

Su M, Fang Y, Li B, Yin W, Gu J, Liang H, Li P, Wu J (2019): Enhanced hexavalent chromium removal by activated carbon modified with micro-sized goethite using a facile impregnation method. Sci Total Environ 647, 47-56

Thiruvenkatachari R, Vigneswaran S, Naidu R (2008): Permeable reactive barrier for groundwater remediation. Journal of Industrial and Engineering Chemistry 14, 145-156

Wang F, Xu W, Xu Z, Liu H (2020): CTMAB-Modified Bentonite–Based PRB in Remediating Cr(VI) Contaminated Groundwater. Water, Air, & Soil Pollution 231

Watson DB, Wu WM, Mehlhorn T, Tang G, Earles J, Lowe K, Gihring TM, Zhang G, Phillips J, Boyanov MI, Spalding BP, Schadt C, Kemner KM, Criddle CS, Jardine PM, Brooks SC (2013): In situ bioremediation of uranium with emulsified vegetable oil as the electron donor. Environ Sci Technol 47, 6440-8

Wei M, Yuan F, Huang G, Chen H, Liu F (2016): Long-term effect of nitrate on Cr(VI) removal by Fe(0): column studies. Environ Sci Pollut Res Int 23, 8589-97

Wen C, Sheng H, Ren L, Dong Y, Dong J (2017): Study on the removal of hexavalent chromium from contaminated groundwater using emulsified vegetable oil. Process Safety and Environmental Protection 109, 599-608

Weng CH, Lin YT, Lin TY, Kao CM (2007): Enhancement of electrokinetic remediation of hyper-Cr(VI) contaminated clay by zero-valent iron. J Hazard Mater 149, 292-302

Xu XR, Li HB, Li XY, Gu JD (2004): Reduction of hexavalent chromium by ascorbic acid in aqueous solutions. Chemosphere 57, 609-13

Yoon IH, Bang S, Chang JS, Gyu Kim M, Kim KW (2011): Effects of pH and dissolved oxygen on Cr(VI) removal in Fe(0)/H2O systems. J Hazard Mater 186, 855-62

Zhang Y, Li Y, Li J, Sheng G, Zhang Y, Zheng X (2012): Enhanced Cr(VI) removal by using the mixture of pillared bentonite and zero-valent iron. Chemical Engineering Journal 185-186, 243-249

Declarations

- Ethics approval and consent to participate (Not applicable)
- Consent for publication (Not applicable)
- Availability of data and materials

The datasets generated during and/or analysed during the current study are not publicly available due to data confidentiality but are available from the corresponding author on reasonable request.

- Competing interests

The authors declare that they have no competing interests.

- Funding

This research was supported by the Program for the Geological Survey of China (No. DD20190354), the National Natural Science Foundation of China (No. 42072276), the National Key Natural Science Foundation of China (No. 41831289).

- Authors' contributions

Conceptualization: Weidong Zhao; Methodology: Weidong Zhao, Lei Ma; Formal analysis and investigation: Weidong Zhao, Xinxiang Huang, Jianshi Gong; Writing - original draft preparation: Xinxiang Huang; Writing - review and editing: Weidong Zhao, Lei Ma; Funding acquisition: Jiazhong Qian, Lei Ma, Weidong Zhao; Resources: Xinxiang Huang; Supervision: Weidong Zhao, Lei Ma.

Figures

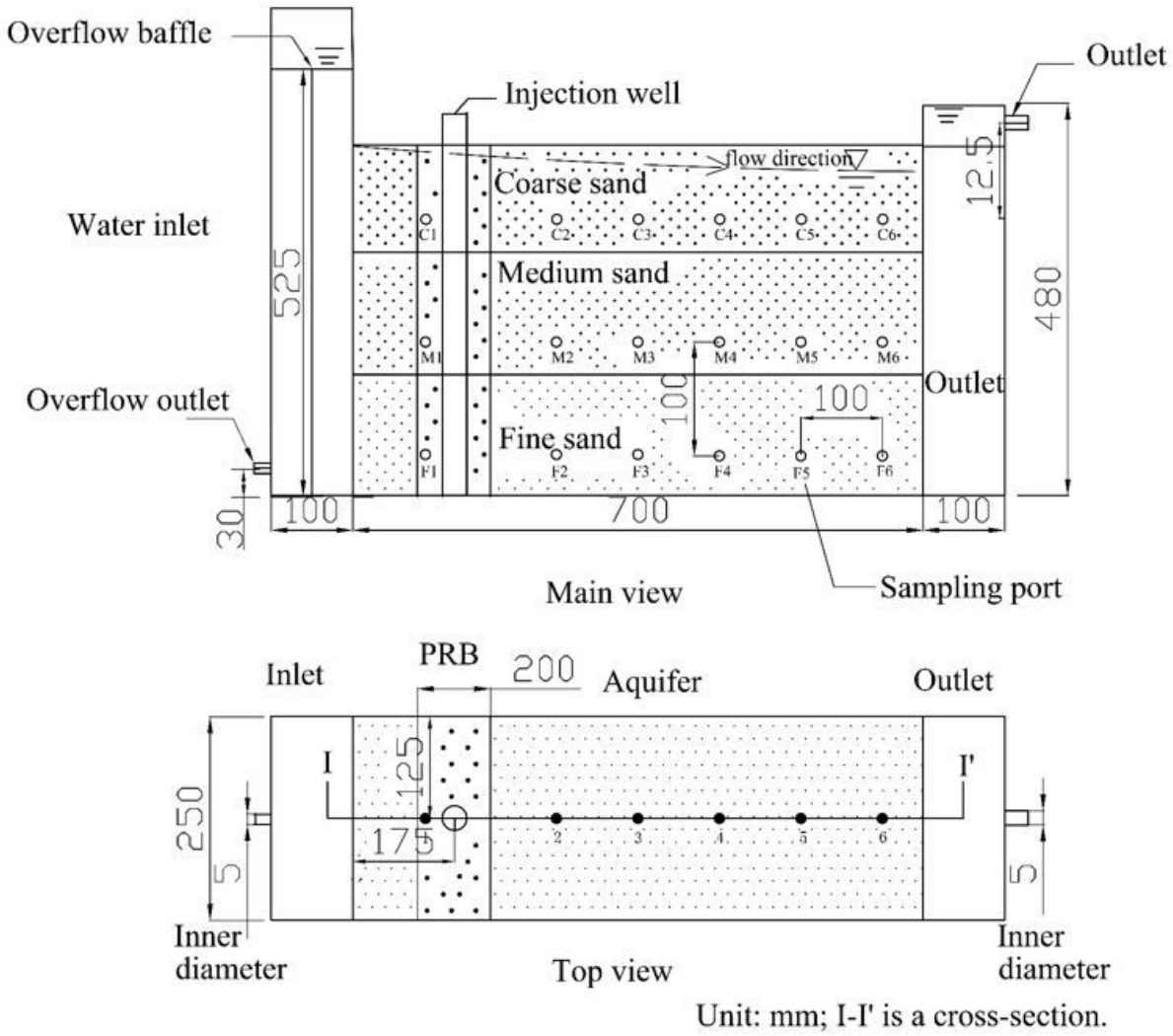

Figure 1

Main view and top view of Cr(VI) diffusion and removal experimental sandbox setup

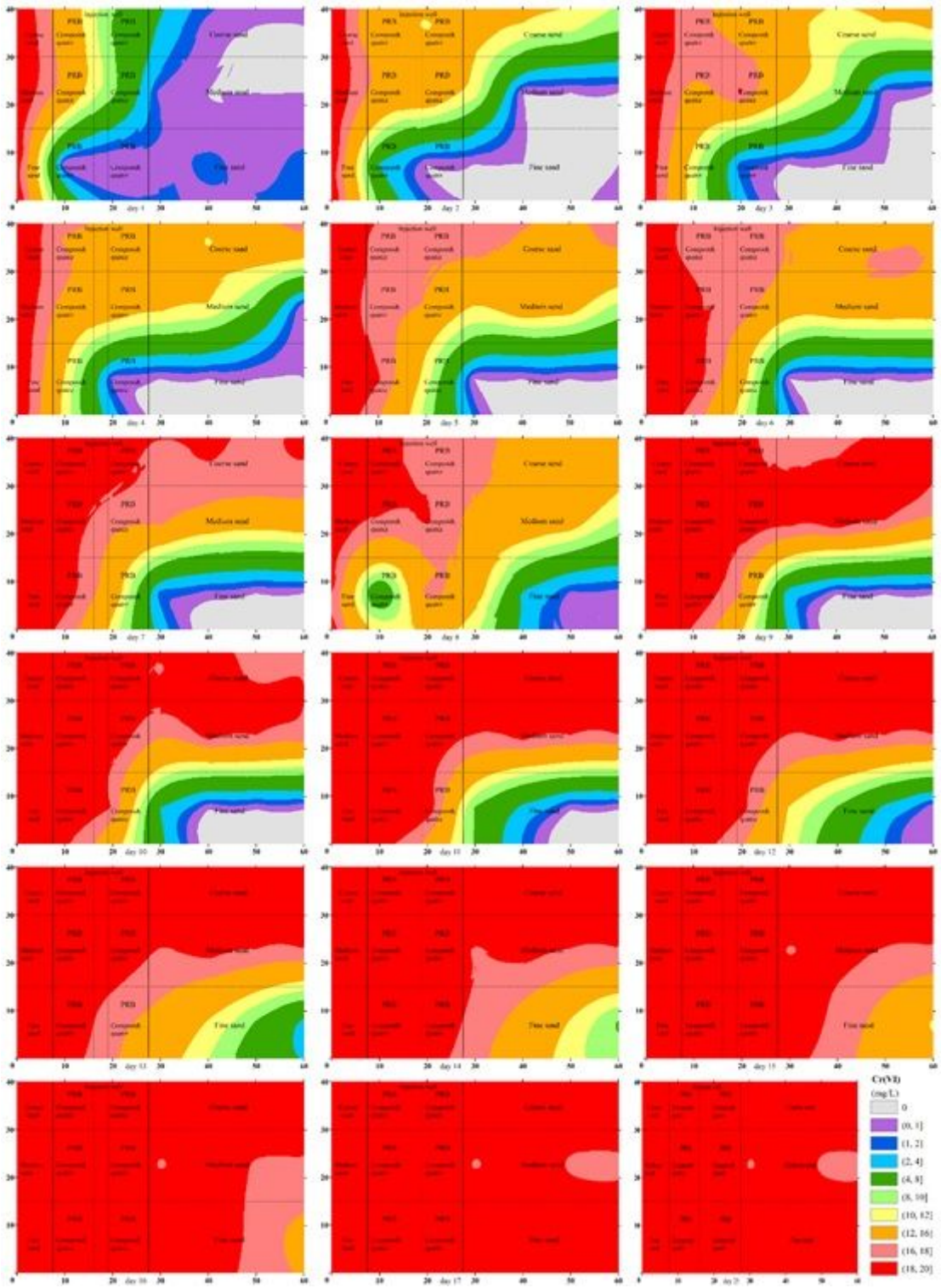

Figure 2

Diffusion of Cr(VI) in the sandbox on different days during stage 1

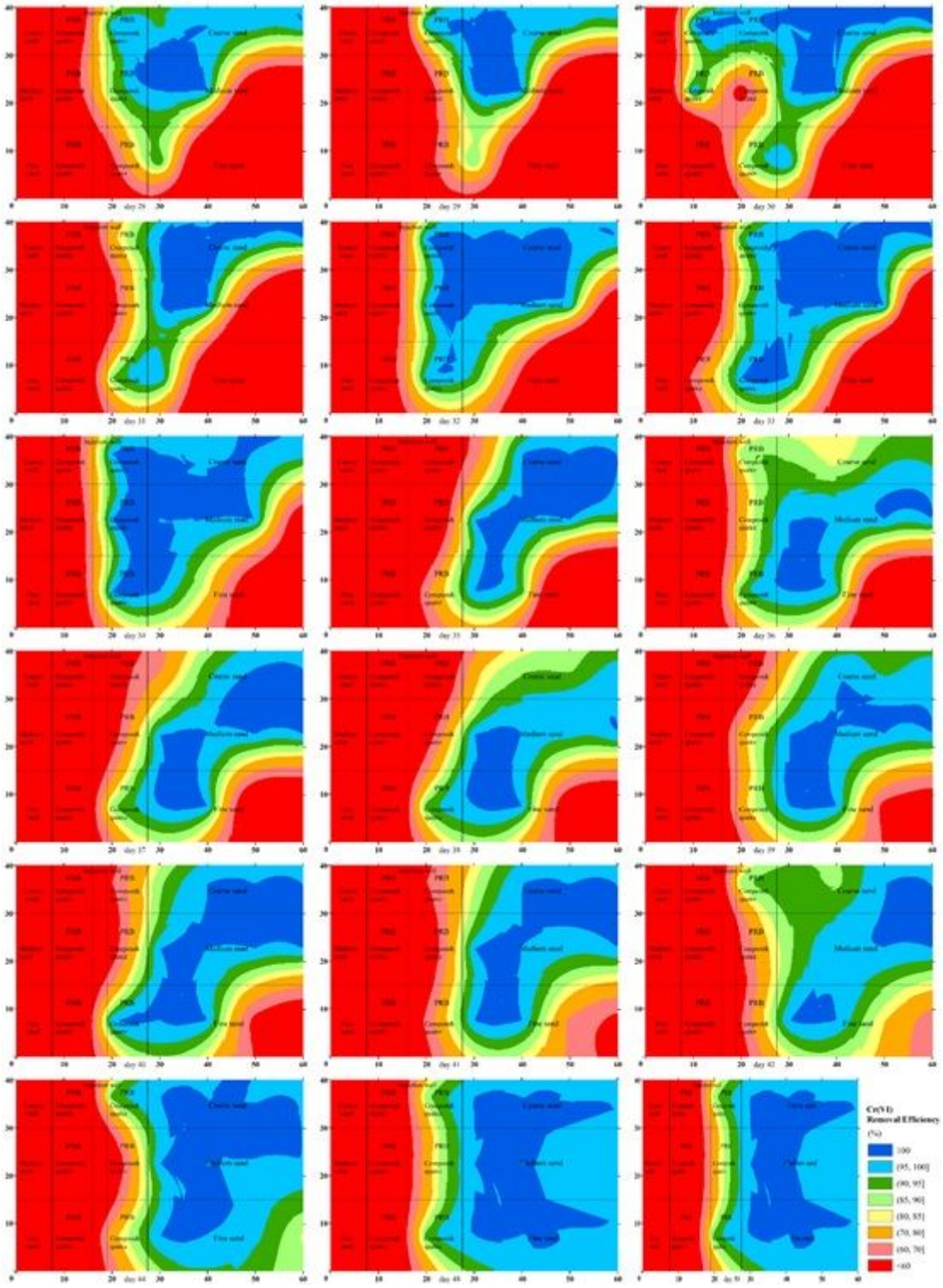

Figure 3

Distribution of Cr(VI) removal efficiency in the sandbox on different days during stage 2

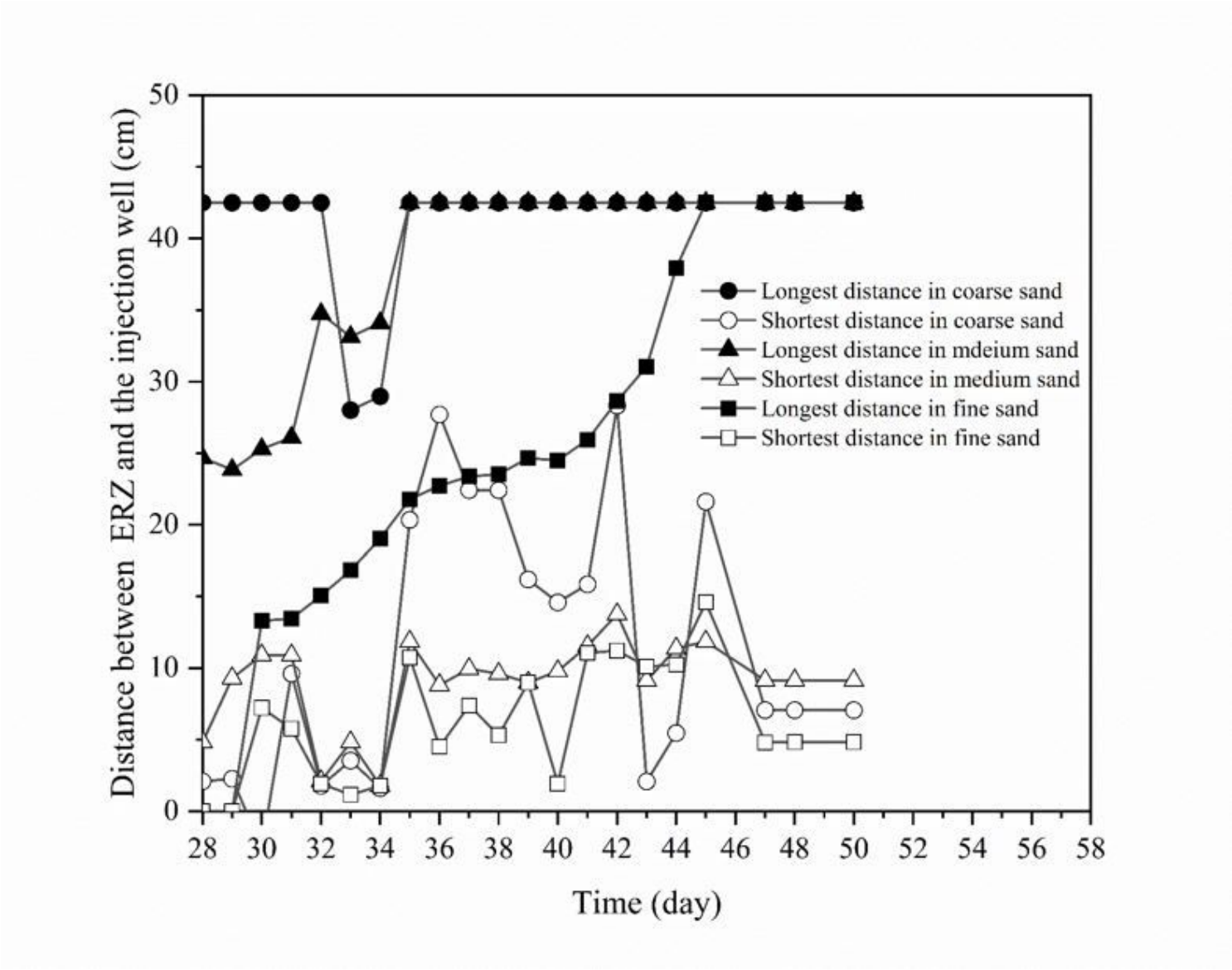

Figure 4

The longest and shortest distances between the ERZ and the injection well in three sand layers during stage 2

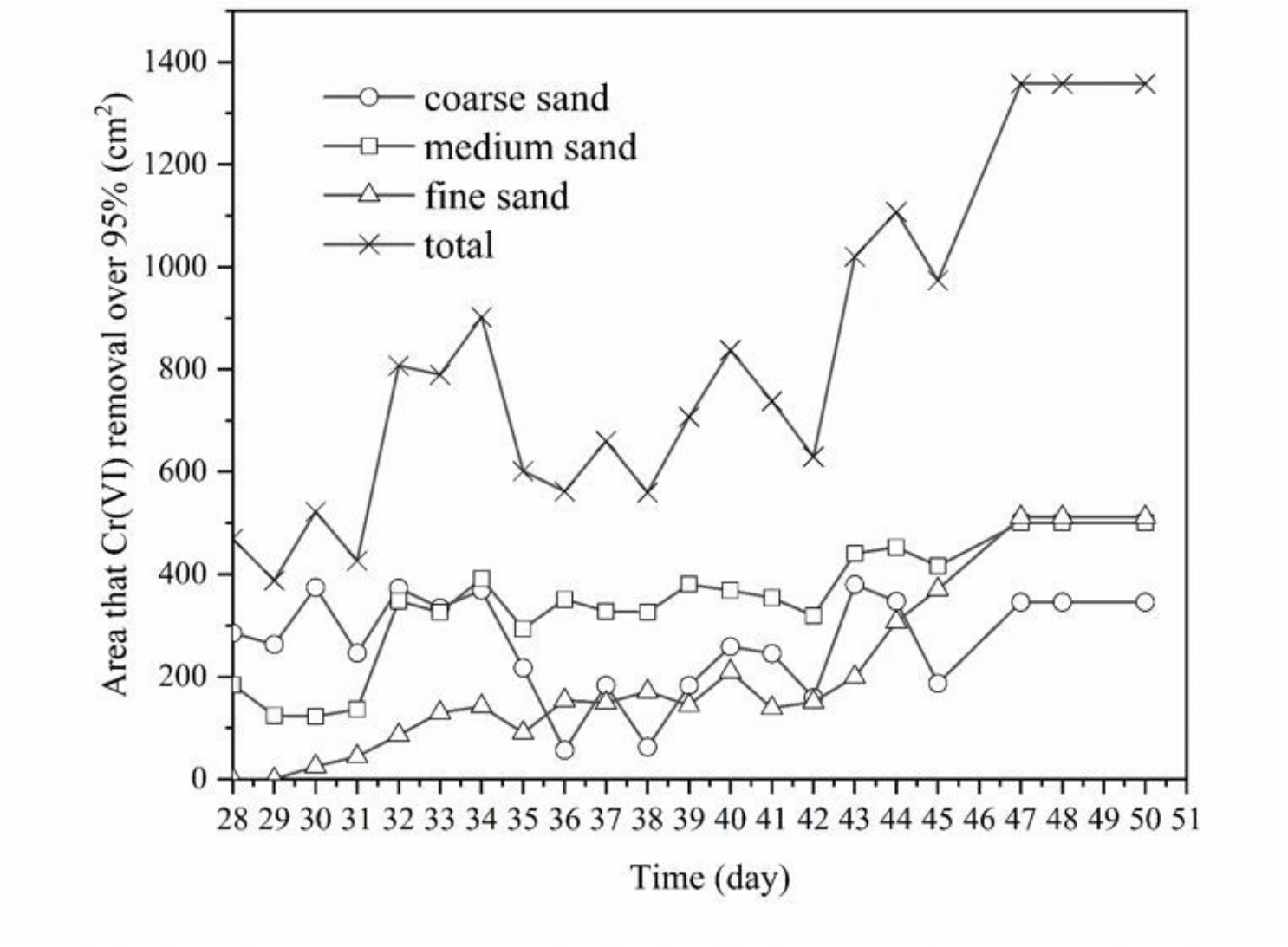

Figure 5

Area change of ERZ in sand layers

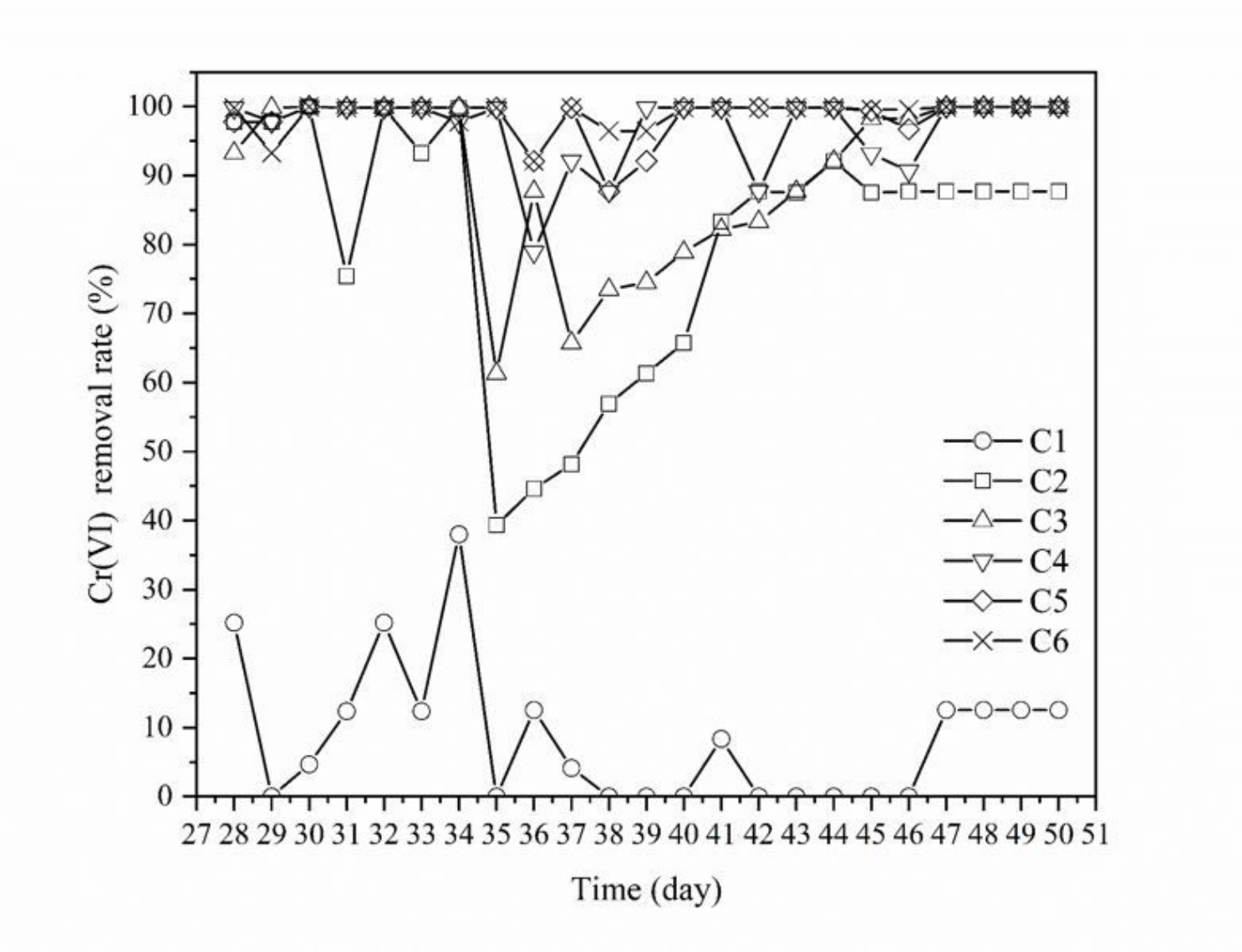

Figure 6

The variation of Cr(VI) removal efficiency in the sampling ports of coarse sand during stage 2 (Cr(VI) = 20 mg/L, 19±0.5 ℃, hydraulic gradient = 3 ‰)

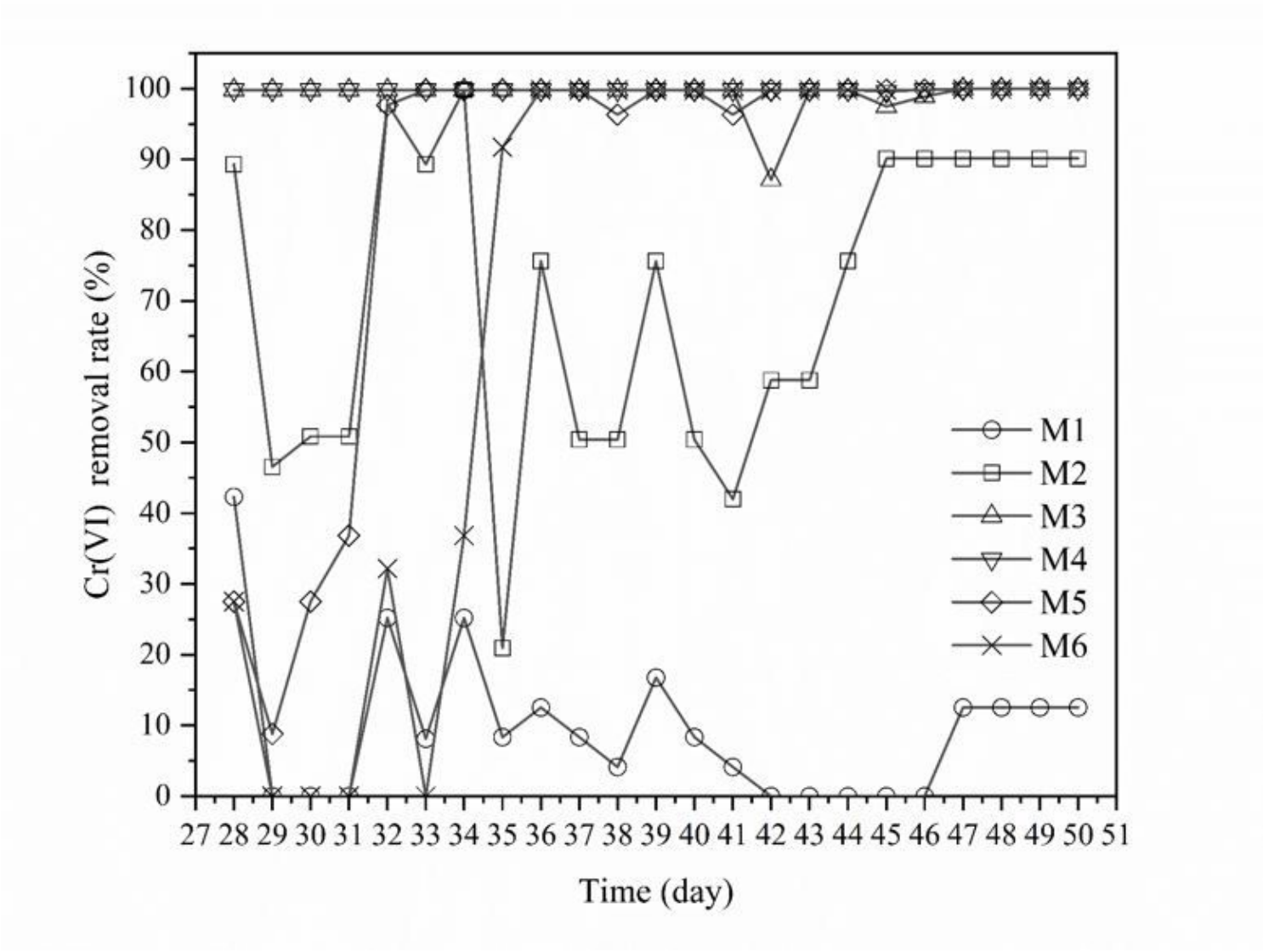

Figure 7

The variation of Cr(VI) removal efficiency in the sampling ports of medium sand during stage 2 (Cr(VI) = 20 mg/L, 19±0.5 ℃, hydraulic gradient = 3 ‰)

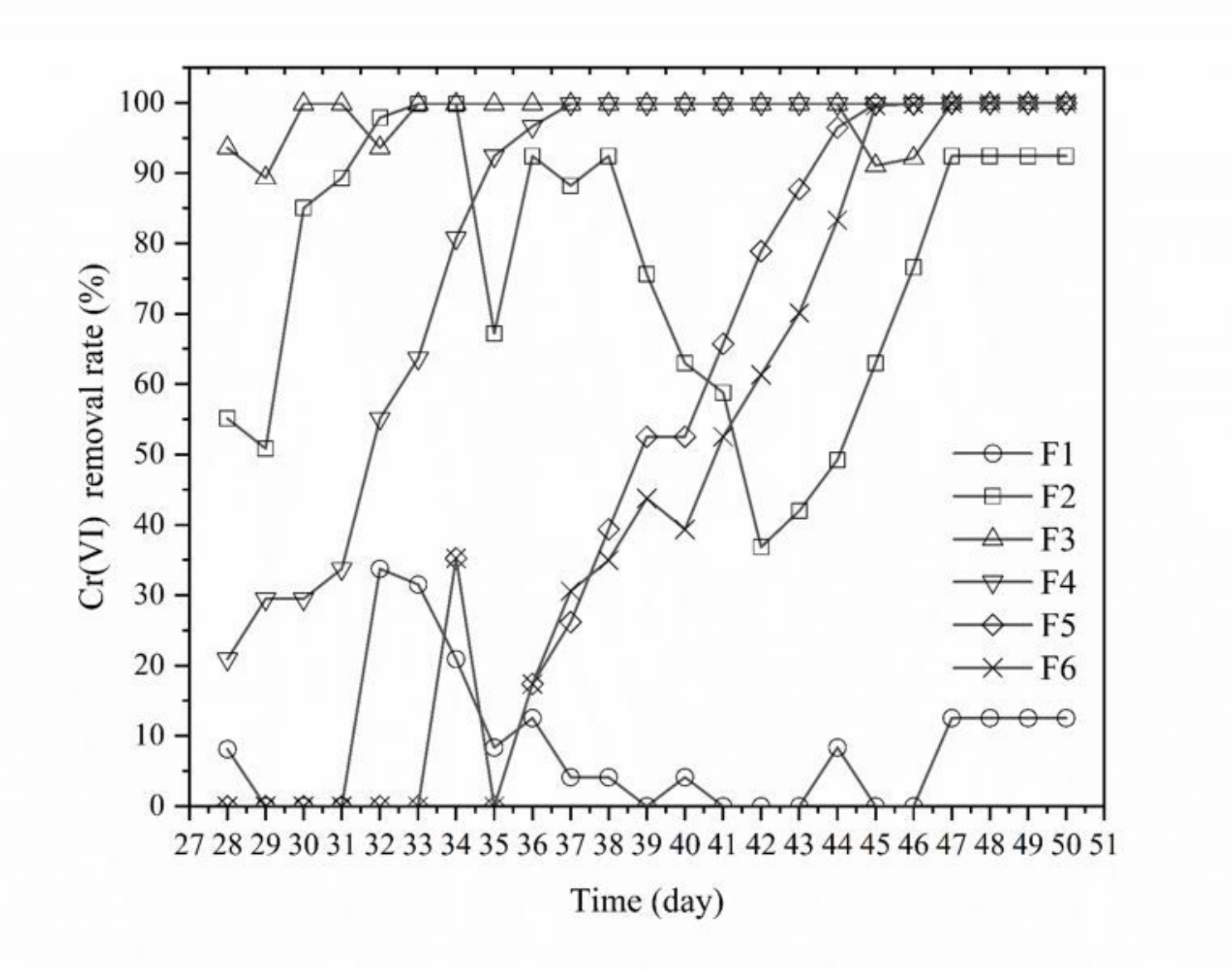

Figure 8

The variation of Cr(VI) removal efficiency in the sampling ports of fine sand during stage 2 (Cr(VI) = 20 mg/L, 19±0.5 ℃, hydraulic gradient = 3 ‰)